the plant journal

SEB Society for Experimental Biology

The Plant Journal (2017) **90,** 918–928 doi: 10.1111/tpj.13518

The genetic architecture of shoot–root covariation during seedling emergence of a desert tree, *Populus euphratica*

Miaomiao Zhang[1,†], Wenhao Bo[1,†], Fang Xu[1,†], Huan Li[1,†], Meixia Ye[1], Libo Jiang[1], Chaozhong Shi[1], Yaru Fu[1], Guomiao Zhao[1], Yuejiao Huang[1], Kirk Gosik[2], Dan Liang[1] and Rongling Wu[1,2,*]

[1]*Center for Computational Biology, College of Biological Sciences and Technology, Beijing Forestry University, Beijing 100083, China, and*

[2]*Center for Statistical Genetics, The Pennsylvania State University, Hershey, PA 17033, USA*

Received 8 November 2016; revised 13 February 2017; accepted 15 February 2017; published online 28 February 2017.
*For correspondence (e-mail rwu@bjfu.edu.cn or rwu@phs.psu.edu).
[†]M.Z., W.B., F.X. and H.L. contributed to this work equally.

SUMMARY

The coordination of shoots and roots is critical for plants to adapt to changing environments by fine-tuning energy production in leaves and the availability of water and nutrients from roots. To understand the genetic architecture of how these two organs covary during developmental ontogeny, we conducted a mapping experiment using Euphrates poplar (*Populus euphratica*), a so-called hero tree able to grow in the desert. We geminated intraspecific F_1 seeds of Euphrates Poplar individually in a tube to obtain a total of 370 seedlings, whose shoot and taproot lengths were measured repeatedly during the early stage of growth. By fitting a growth equation, we estimated asymptotic growth, relative growth rate, the timing of inflection point and duration of linear growth for both shoot and taproot growth. Treating these heterochronic parameters as phenotypes, a univariate mapping model detected 19 heterochronic quantitative trait loci (*h*QTLs), of which 15 mediate the forms of shoot growth and four mediate taproot growth. A bivariate mapping model identified 11 pleiotropic *h*QTLs that determine the covariation of shoot and taproot growth. Most QTLs detected reside within the region of candidate genes with various functions, thus confirming their roles in the biochemical processes underlying plant growth.

Keywords: growth equation, quantitative trait loci, functional mapping, *Populus euphratica*, shoot–root relationship.

INTRODUCTION

Plant growth is a biological process highly affected by the coordination of above-ground shoots and below-ground roots that operates through energy production in leaves in response to the availability of water and nutrients (Paul and Foyer, 2001). By light capturing and carbon assimilation, the shoots transport photosynthetic products to the roots (Gartner, 1995), whereas the roots supply a variety of growth substances for the shoots through water and nutrient foraging (Reich, 2002). Several theories, such as the balanced growth hypothesis (Shipley and Meziane, 2002) or functional equilibrium hypothesis (Brouwer, 1963; Poorter *et al.*, 2012), have been proposed to interpret the phenomenon of why more biomass is allocated to those organs that are responsible for acquiring the limiting resources. Several studies have begun to study the molecular mechanisms underlying shoot–root balancing. More recently, Chen *et al.* (2016) have identified a bZIP transcription factor ELONGATED HYPOCOTYL5 (HY5) that serves as a shoot–root mobile signal to mediate light-regulated coupling of shoot growth and C assimilation with root growth and N uptake. However, we still know little about the overall genetic underpinnings that govern the interaction and coordination of shoot and root growth in plants, especially in forest trees.

Quantitative trait loci (QTL) mapping, aimed to map the underlying genes to particular chromosomal locations, is a powerful approach for drawing the overall picture of the genetic architecture of complex traits (Lander and Botstein, 1989; Wu *et al.*, 2007; Miles and Wayne, 2008). This approach has been utilized to dissect growth-related traits of shoots and roots in wheat (Bai *et al.*, 2013), wild barley (Naz *et al.*, 2014), maize (Ruta *et al.*, 2010), potato

(Anithakumari *et al.*, 2011; Khan *et al.*, 2015) and *Arabidopsis thaliana* (El-Lithy *et al.*, 2010; Bouteille *et al.*, 2012). Because most traits associated with growth and development can be better described by a dynamic process (Hernandez, 2015; Muraya *et al.*, 2017), it is more biologically meaningful to map these traits as growth curves (Sun and Wu, 2015). Several approaches have integrated growth equations into the likelihood of genetic mapping, leading to the birth of a so-called functional mapping model (Ma *et al.*, 2002; Wu and Lin, 2006; Li and Sillanpaa, 2015; Muraya *et al.*, 2017). Functional mapping allows the developmental change of genetic architecture to be characterized across time and space (He *et al.*, 2010; Li and Wu, 2010). By modeling the longitudinal mean-covariance structures using a set of parsimonious parameters, functional mapping has proven to have great statistical power in gene identification and the utilization of sparse phenotypic data (Hou *et al.*, 2005, 2006). An alternative to functional mapping is to map growth QTLs by estimating growth parameters for each genotype based on growth equations and associating these parameters with markers (Wu *et al.*, 2002). This alternative has been used to map the developmental pattern of leaf size and shape in *Brassica rapa* (Baker *et al.*, 2015). All these approaches implement the mathematical aspect of developmental principles into a mapping setting, thereby gleaning new biological insight and robust statistical power (Hernandez, 2015).

In this article, we report the results of the genetic architecture of the developmental dynamics of shoot–root relationships in Euphrates Poplar (*Populus euphratica* Oliv.). As the only woody plant species that can grow in the harsh desert, *P. euphratica* has many desirable properties for ecophysiological studies of growth allocation, such as high tolerance to extreme temperature, salinity, drought and wind, and considerable variability in such tolerance (Ferreira *et al.*, 2008; Si *et al.*, 2014). Our study was based on a full-sib family of 370 genotyped members derived from two different trees sampled from a natural stand in northwestern China. These full-sib seeds were germinated into seedlings in isolated tubes. Germination and seedling establishment are crucial stages to the life cycle of plants, which exert a profound influence on the subsequent development (Verma *et al.*, 2015). Different from traditional mapping approaches based on phenotypes measured at single time points, we used the growth parameters-based mapping model to study the genetic architecture of the form and pattern of above- and below-ground growth in Euphrates poplars by measuring the growth at a series of time points. By fitting a logistic growth equation that best fits growth trajectories of shoot and root length for each F_1 seedling, we obtained the estimates of a set of growth parameters for all progeny and further applied these estimates as phenotypes for QTL mapping.

RESULTS

Growth parameters

The growth equation (1) was found to fit the longitudinal data of shoot length (Figure S1) and taproot lengths for each progeny well (Figure S2). By using a non-linear least-squares approach, we obtained the estimates of three growth parameters and the standard errors of these parameter estimates in each case (Table S1). Reasonably low estimation errors, along with the independence of model residuals from time points, show the statistical robustness of equation fitness (Figure S3). Following Sun *et al.*'s developmental model, we calculated and chose four key heterochronic parameters, asymptotic growth (a), relative growth rate (r), the timing of inflection point (T_I) and the duration of linear growth (L) as phenotypic values to perform QTL mapping. A great variability was observed for growth curve parameters of both phenotypic traits (Table 1). Compared with taproot length, shoot length has a greater rate of growth and reaches the maximum growth rate at an earlier time. However, shoot length experiences a shorter period of linear growth than taproot length growth. All these indicate that different patterns of growth have emerged for above- and below-ground components in Euphrates Poplars during their early stage of development.

Figure 1 illustrates the correlation pattern among four heterochronic parameters within and between traits. It was found that growth parameters are more strongly correlated with each other within traits than between traits, suggesting evidence of developmental modularity. The asymptotic growth displays remarkable positive correlations with

Table 1 Averages of the estimates of heterochromic parameters (a, r, t_I and L), their standard deviations and ranges for shoot length and taproot length in the F_1 population of Euphrates poplars

Parameter	a	r	t_I	L
Mean				
Shoot length (mm)	94.926 ± 2.898	0.082 ± 0.001	84.565 ± 0.926	33.640 ± 0.433
Taproot length (mm)	487.686 ± 39.240	0.074 ± 0.002	88.643 ± 1.831	40.475 ± 0.716
Range				
Shoot length (mm)	3.042–290.594	0.027–0.136	36.479–219.928	19.354–98.648
Taproot length (mm)	11.575–4843.135	0.024–0.216	28.522–214.445	12.194–110.267

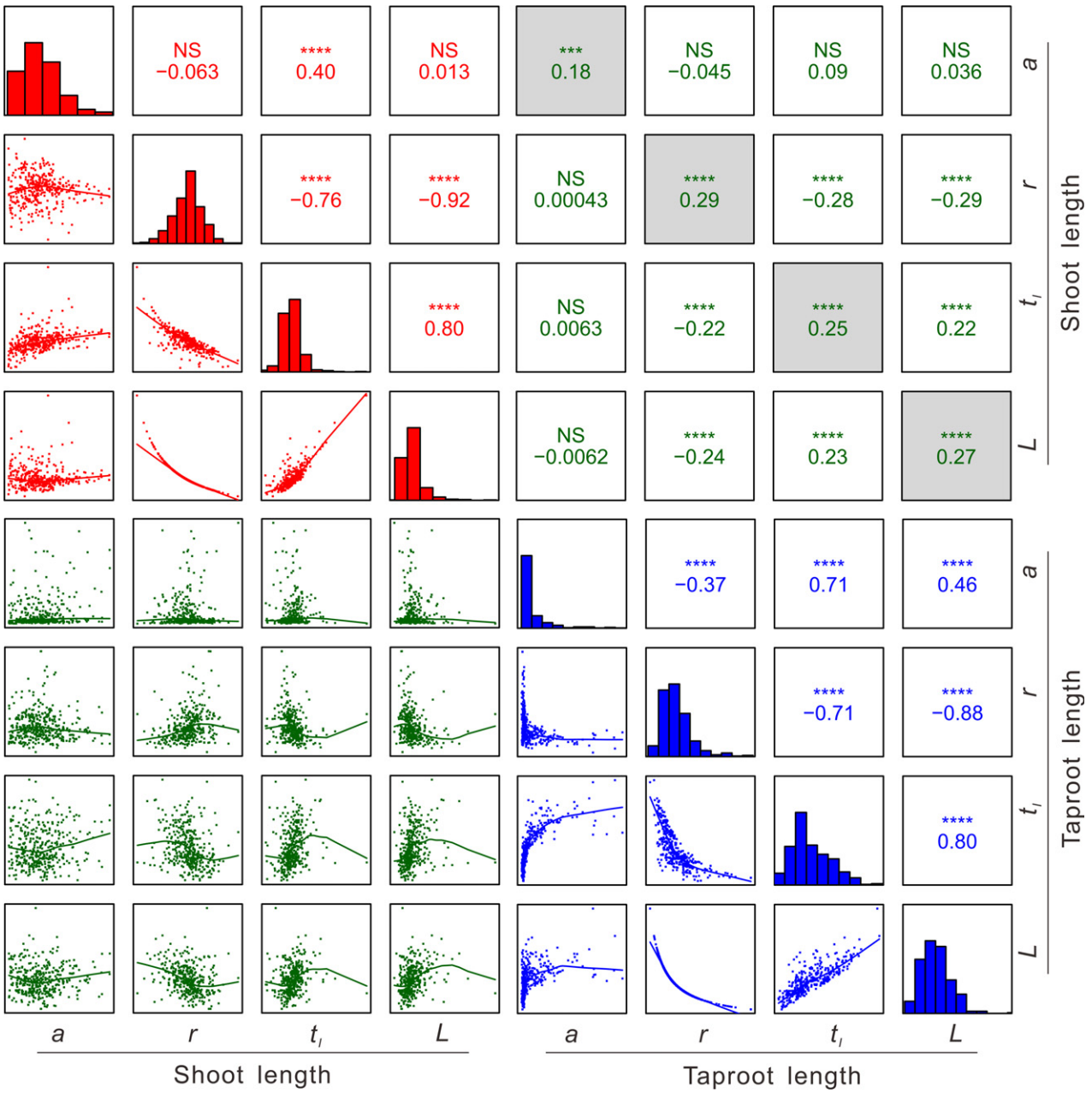

Figure 1. Scatter plots (lower triangle) and correlations (upper triangles) among four heterochronic parameters of shoot and taproot length growth in the F_1 mapping population of *Populus euphratica*. [Colour figure can be viewed at wileyonlinelibrary.com]

growth rate, the timing of inflection point and the duration of linear growth for both above- and below-ground traits. Growth rate is negatively correlated with the timing of inflection point, suggesting that fast-growing progeny usually delay their time to reach maximum growth rate.

*h*QTL identification and gene ontology

The QTLs that affect heterochronic parameters are defined as heterochronic QTLs or hQTLs (Sun *et al.*, 2014; Jiang *et al.*, 2015). We first used the univariate mapping model to analyze each heterochronic parameter for individual traits. Of a total of 19 significant SNPs, identified as *h*QTLs, after Bonferroni correction ($P < 0.05$), 15 are related with shoot length parameters and four with taproot length parameters (Table 2). It is interesting to see that the 12 *h*QTLs detected for the asymptotic growth of shoot length are located on linkage group 12, of which three are tightly linked together at a narrow interval 81.5–81.9 cM , two at 122.8 cM and three at a narrow interval 209.4–212.6 cM (Figures 2 and S4). Two *h*QTLs for growth rate and one *h*QTL for the duration of linear growth for shoot length were located on linkage groups 5 and 18, respectively.

Table 2 The chromosomal positions, cross-types and heritabilities of significant QTLs detected by a univariate analysis to affect heterochronic parameters of the shoot length and taproot length growth in the F_1 mapping population of *Populus euphratica*

Trait	Marker ID	Gene ID	Linkage group	Genetic distances (cM)	Heritability (%)	Cross-type	Allele	Description
Shoot length								
a								
1	hk_hk_1929	105110031	12	81.49	8.21	Intercross	[T/C]	*Populus euphratica* cation/H(+) antiporter 24 (LOC105110031), mRNA
2	nn_np_6534		12	81.5	5.77	Testcross	[C/T]	
3	nn_np_8676	105110064	12	81.94	6.04	Testcross	[C/T]	*Populus euphratica* probable protein phosphatase 2C 26 (LOC105110064), transcript variant X4, misc_RNA
4	nn_np_6447	147815418	12	122.80	6.67	Testcross	[T/A]	*Vitis vinifera* contig VV78X127459.6, whole genome shotgun sequence
5	hk_hk_1831	7472131	12	122.81	5.99	Intercross	[G/C]	*Populus trichocarpa* nodulin family protein (POPTR_0009s13530 g) mRNA, complete cds
6	nn_np_3806		12	141.35	5.66	Testcross	[A/C]	
7	hk_hk_1786	105141875	12	209.35	5.91	Intercross	[C/G]	*Populus euphratica* uncharacterized LOC105141875 (LOC105141875), mRNA
8	hk_hk_899	48209782	12	211.64	8.18	Intercross	[C/A]	*Populus trichocarpa* clone Pop1-16J18, complete sequence
9	hk_hk_1546	105108052	12	212.61	8.70	Intercross	[C/G]	*Populus euphratica* uncharacterized LOC105108052 (LOC105108052), transcript variant X2, mRNA
10	hk_hk_1680	105108436	12	218.27	5.42	Intercross	[A/C]	*Populus euphratica* leucine-rich repeat receptor-like protein kinase PEPR1 (LOC105108436), mRNA
11	hk_hk_1331	105108534	12	218.28	7.35	Intercross	[C/T]	*Populus euphratica* RNA pseudouridine synthase 4, mitochondrial (LOC105108534), transcript variant X2, mRNA
12	hk_hk_1037		12	246.75	5.92	Intercross	[C/T]	
r								
1	lm_ll_4882	105113529	5	4.96	5.88	Testcross	[C/T]	*Populus euphratica* probable F-box protein At4 g22030 (LOC105113529), mRNA
2	lm_ll_6547	105108183	5	15.38	5.74	Testcross	[T/G]	*Populus euphratica* polyadenylation and cleavage factor homolog 4-like (LOC105108183), mRNA
L								
1	lm_ll_3826	105127456	18	123.7	9.89	Testcross	[T/C]	*Populus euphratica* uncharacterized LOC105127456 (LOC105127456), ncRNA
Taproot length								
a								
1	hk_hk_830		9	83.97	7.50	Intercross	[C/T]	*Solanum pennellii* chromosome ch11, complete genome
2	hk_hk_937	18102890	9	84.21	7.24	Intercross	[T/C]	*Populus trichocarpa* hypothetical protein (POPTR_0011s01954 g) mRNA, complete cds
r								
1	hk_hk_371		6	92.07	5.75	Intercross	[A/G]	
t_1								
1	nn_np_5611	105123565	9	135.23	5.63	Testcross	[A/T]	*Populus euphratica* pentatricopeptide repeat-containing protein At4 g14850/LOI1 (LOC105123565), mRNA

Gene annotations of QTLs were also given.

Linkage group 9 harbors three significant *h*QTLs, of which two highly linked at a narrow interval 84.0–84.2 cM affect the asymptotic growth of taproot length and one at a different location affects the timing of inflection point for the same trait. Only one *h*QTL for the growth rate of taproot length was detected on linkage group 6. Different sets

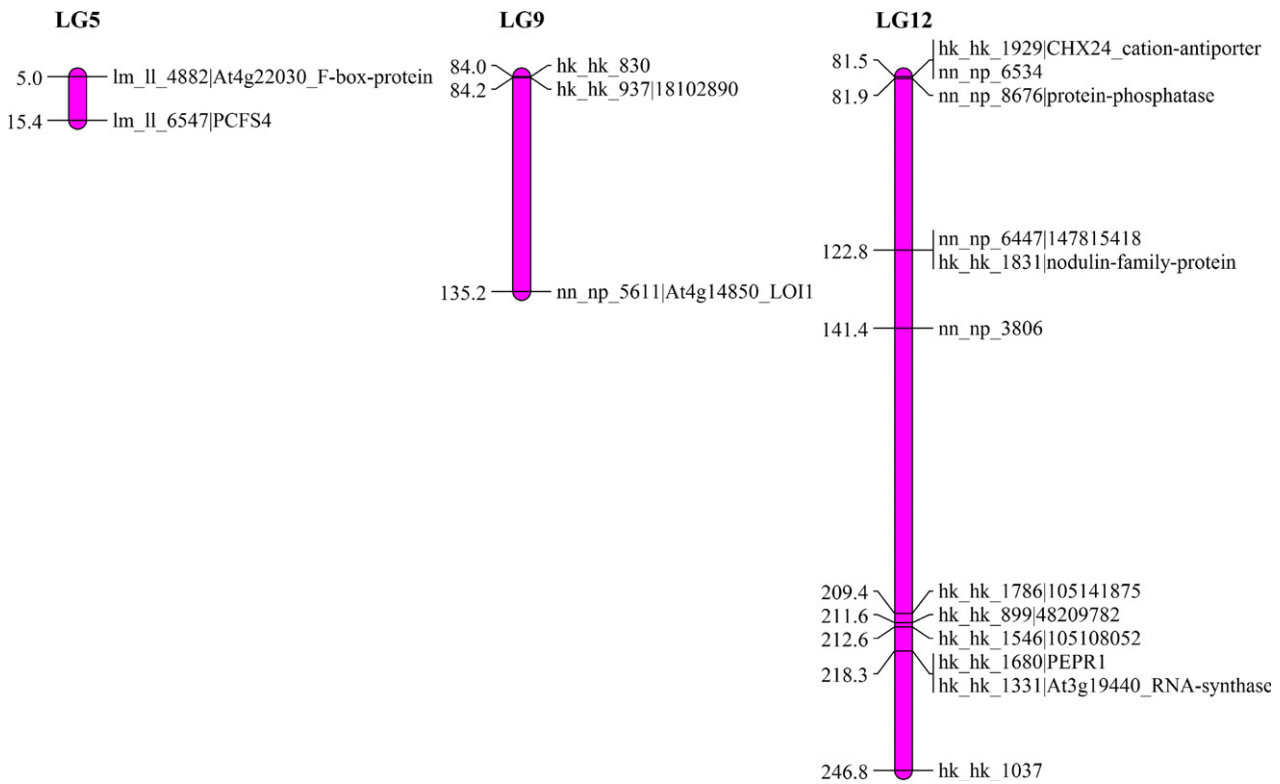

Figure 2. Diagrammatic genomic positions of several significant quantitative trait loci (QTLs) detected for heterochronic parameters of shoot and taproot length growth. [Colour figure can be viewed at wileyonlinelibrary.com]

of SNPs on heterochronic parameters of shoot length and taproot length indicate that these two traits present different modules during development. Each detected *h*QTL was observed to explain heritabilities ranging from 5.42% to 9.89% (Table 2).

The analysis of gene annotations through GenBank, UniProt and STRING identified 15 putative homologous genes in the genomes of *P. euphratica*, *Populus trichocarpa, Vitis vinifera* L. and *Solanum pennellii*, among which eight *h*QTL have retained functional annotations (Table 2). They primarily participate in cation transportation, protein phosphorylation, nodule formation, RNA synthase, mRNA maturation, isoprenoid biosynthesis, plant defense, hormone signal transduction and other biological developmental processes (Tables 2). The remaining seven *h*QTL did not give detailed information. Specifically, three of them were not clear about the functional annotations, which could be blasted on the genome of *P. trichocarpa, V. vinifera* L. and *S. pennellii*; three *h*QTL (hk_hk_1546, hk_hk_1786 and nn_np_3826) could code uncharacterized mRNA and ncRNA in *P. euphratica*; one *h*QTL (hk_hk_937) could code hypothetical protein (POPTR_0011s01954 g) in *P. trichocarpa*.

For the eight *h*QTL that have retained functional annotations, the nn_np_8676, a miscellaneous RNA (misc RNA), is probable protein phosphatase 2C 26 (LOC105110064) in *P. euphratica*. The hk_hk_1831, an mRNA, may code nodulin family protein (POPTR_0009s13530 g) in *P. euphratica*. The hk_hk_1929 may operate antiporter activity and solute: proton antiporter activity as CHX24 with coding for cation/H^+ antiporter, which participates in the processes of ion transport, cation transport, potassium ion transport, transmembrane transport, hydrogen ion transmembrane transport and the regulation of pH. The cation/H^+ antiporter is a component of the endomembrane system, and integral component of the membrane. The lm_ll_6547 was predicted to be a gene of PCFS4 coding the protein of polyadenylation and leverage factor homolog 4, which is a component of the nucleus, cytoplasm and mRNA cleavage factor complex. PCFS4 plays a role in several plant developmental and biochemical processes, including termination of RNA polymerase II transcription, mRNA polyadenylation, mRNA cleavage, mRNA processing, flower development and positive regulation of flower development, with the function of RNA polymerase II core binding, mRNA binding, and metal ion binding. The hk_hk_1680 is a putative gene of PEPR1, which codes leucine-rich repeat receptor-like protein kinase, a component of plasma membrane, plasmodesma, membrane, and integral component of the membrane. PEPR1 plays a key role in many plant biological processes, such as cGMP biosynthetic process, protein phosphorylation, defense response,

immune response, signal transduction, response to wounding, response to jasmonic acid, phosphorylation and innate immune response, with the functions of nucleotide binding, peptide receptor activity, guanylate cyclase activity, protein kinase activity, protein serine/threonine kinase activity, protein binding, ATP binding, kinase activity and transferase activity. The lm_ll_4882 is the probable F-box protein (At4g22030), which participates in the process of proteasome-mediated ubiquitin-dependent protein catabolic as a component of ubiquitin ligase complex. The hk_hk_1331 (At3g19440) may code RNA pseudouridine synthase 4 as a component of the mitochondrion. This gene participates in pseudouridine synthesis, RNA modification and tRNA pseudouridine synthesis, with the function of RNA binding, pseudouridine synthase activity, isomerase activity and deaminase activity. Interestingly, we detected the gene of nn_np_5611, which is homologeous with the gene LOI1 (At4 g14850), which is also a component of the mitochondrion. LOI1 codes pentatricopeptide repeat-containing protein, which participates in sterol metabolic process, isopentenyl diphosphate biosynthetic process (mevalonate pathway), isopentenyl diphosphate biosynthetic process (methylerythritol 4-phosphate pathway), root development and regulation of catalytic activity, with the functions of nucleotide binding, RNA binding, zinc ion binding and poly(G) binding.

We also obtained the interactive proteins and interaction networks for At3g19440 and LOI1 in *A. thaliana* by the software STRING (Figure 3; Tables S2 and S3). As the RNA pseudourine synthase 4, At3g19440 can interact with multiple genes associated with important compounds synthesis, including TOPII, At3g23145, At4 g10320, RIBA2, and even including a photosensitive gene T21L8.140 (Figure 3a; Table S2). Functional enrichments results showed that At3g19440 participates in multiple biosynthetic and metabolic processes, affects activity and binding of other biomolecules, and plays a key role in two KEGG pathways of riboflavin metabolism and aminoacyl-tRNA biosynthesis (Table S3). LOI1 works as a regulatory factor of isoprenoid biosynthesis, and the result of protein–protein interactive network showed that LOI1 could also affect other biosynthesis processes, such as ATPQ for ATP synthesis, AT5G15700 for RNA polymerization (Figure 3b). LOI1 also interacts with MEF14 for mitochondrial editing and three genes related to the cytochrome complex (cytochrome c), which is capable of undergoing oxidation and reduction as an essential component of the electron transport chain (Table S2). LOI1 participates in a KEGG pathway of oxidative phosphorylation, and is active in the mitochondrion, organelle envelope and cytoplasm (Table S3). It should be noted that in a few cases highly linked SNPs can each be annotated to a different gene, presenting a possibility of multiple co-localized QTLs for the same traits (Figures 2 and S4).

Pleiotropic effect of shoot–taproot growth

To investigate how an *h*QTL affects above- and below-ground parts of juvenile Euphrates Poplars, we employed the bivariate mapping model to analyze each pair of heterochronic parameters for shoot length and taproot length. The model detected eight *h*QTLs for the asymptotic growth of these two traits (Table 3). Through hypothesis tests on the two traits, respectively, we found that all these *h*QTLs are pleiotropic, exhibiting significant effects on both shoot length and taproot length. However, these pleiotropic *h*QTLs do not exert the same magnitudes of effects on the two traits, of which six contribute more substantially to shoot length than taproot length (5.74–8.70% versus 0.72–7.24%), whereas the other two contribute in an inverse pattern (1.97 versus 7.50% and 1.02 versus 1.10%).

A pleiotropic testcross *h*QTL for the growth rate of shoot length and taproot length was mapped to linkage group 5, although it explains much more variance for the former than the latter (5.31 versus 0.01%; Table 3). It is interesting

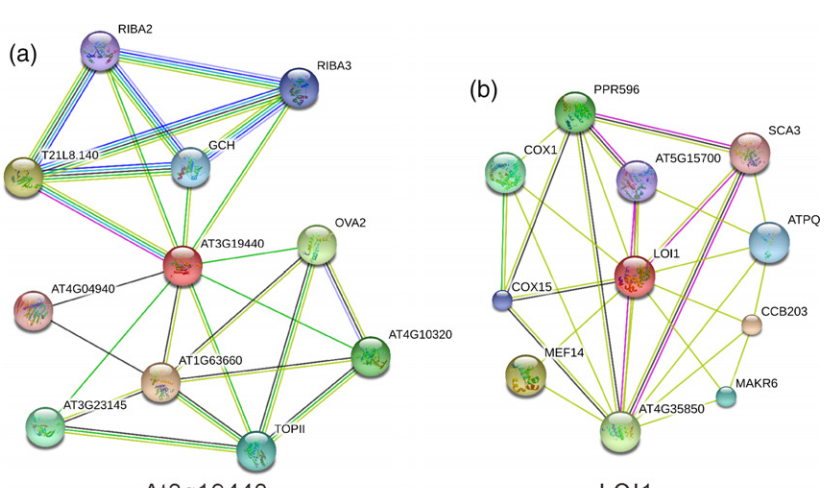

Figure 3. Interaction network of At3 g19440 (a) and LOI1 (b) in *Arabidopsis thaliana.* [Colour figure can be viewed at wileyonlinelibrary.com]

Table 3 The chromosomal positions, cross-types and heritabilities of significant QTLs detected by a bivariate analysis to affect heterochronic parameters of the shoot length and taproot length growth in the F_1 mapping population of *Populus euphratica*

Trait	Marker ID	Gene ID	Linkage group	Genetic distances (cM)	Heritability (%)	Cross-type	Allele	Description
a								
1	hk_hk_1929	105110031	12	81.49	5.91 0.72	Intercross	[T/C]	*Populus euphratica* cation/H(+) antiporter 24 (LOC105110031), mRNA
2	hk_hk_830		9	83.97	1.97 7.50	Intercross	[C/T]	*Solanum pennellii* chromosome ch11, complete genome
3	hk_hk_937	18102890	9	84.21	8.21 7.24	Intercross	[T/C]	*Populus trichocarpa* hypothetical protein (POPTR_0011s01954 g) mRNA, complete cds
4	nn_np_6447	147815418	12	122.8	1.02 1.10	Testcross	[T/A]	*Vitis vinifera* contig VV78X127459.6, whole genome shotgun sequence
5	hk_hk_1786	105141875	12	209.35	8.18 1.91	Intercross	[C/G]	*Populus euphratica* uncharacterized LOC105141875 (LOC105141875), mRNA
6	hk_hk_899	48209782	12	211.64	8.70 2.32	Intercross	[C/A]	*Populus trichocarpa* clone Pop1-16J18, complete sequence
7	hk_hk_1546	105108052	12	212.61	7.35 3.26	Intercross	[C/G]	*Populus euphratica* uncharacterized LOC105108052 (LOC105108052), transcript variant X2, mRNA
8	hk_hk_1331		12	218.28	5.74 1.08	Intercross	[C/T]	*Populus euphratica* RNA pseudouridine synthase 4, mitochondrial (LOC105108534), transcript variant X2, mRNA
r								
1	lm_ll_6547	105108183	5	15.38	5.31 0.01	Testcross	[T/G]	*Populus euphratica* polyadenylation and cleavage factor homolog 4-like (LOC105108183), mRNA
L								
1	lm_ll_6547	105108183	5	15.38	9.89 0.34	Testcross	[T/G]	*Populus euphratica* polyadenylation and cleavage factor homolog 4-like (LOC105108183), mRNA
2	lm_ll_3826	105127456	18	123.7	1.10 1.35	Testcross	[T/C]	*Populus euphratica* uncharacterized LOC105127456 (LOC105127456), ncRNA

Gene annotations of QTLs were also given.

to note that, although taproot length displays a much smaller genotype-dependent difference in growth rate than shoot length, two genotypes at this *h*QTL converge to substantially more different asymptotic values for taproot length than shoot length (Figure 4). This *h*QTL was also found to pleiotropically affect the timing of inflection point and the linear growth duration of these two traits. For both of these heterochronic parameters, the *h*QTL exerts a larger genetic effect on and explains a larger proportion of the phenotypic variance for taproot length than shoot length (Figure 4; Table 3). Gene annotation shows this *h*QTL resides in the homolog 4-like polyadenylation and cleavage factor (LOC105108183). A second pleiotropic *h*QTL for the linear growth duration of shoot length and taproot length was found on linkage group 18, nearby an uncharacterized LOC105127456 ncRNA-coding gene.

DISCUSSION

A long-standing question of fundamental importance to plant ecophysiologists is how plants allocate their biomass to different organs in order to achieve the economic use of resources and maximum functionality and fitness (Shipley and Meziane, 2002). The 'balanced growth' hypothesis states that a plant would allocate more biomass to the organs responsible for acquiring limiting resources (Brouwer, 1963; Shipley and Meziane, 2002; Poorter *et al.*, 2012). As the only woody plant that can survive and reproduce in the desert, Euphrates Poplars have evolved the capacity of developing a deep taproot even at its stage of seed germination, and they can maintain this capacity as trees age (Liu *et al.*, 2015; Wang *et al.*, 2015). This hypothesis was well confirmed by our experiment of Euphrates Poplar seedlings in which the below-ground shoot growth was found to be strikingly larger than the above-ground Taproot growth (Table 1). On average, the asymptotic growth of taproot length was fourfold larger than that of shoot length during the germination process of Euphrates Poplar.

To quantify the genetic and developmental mechanisms of growth allocation, we developed and applied mathematical models to dissect growth trajectories of shoot length and taproot length, and integrated these models into a

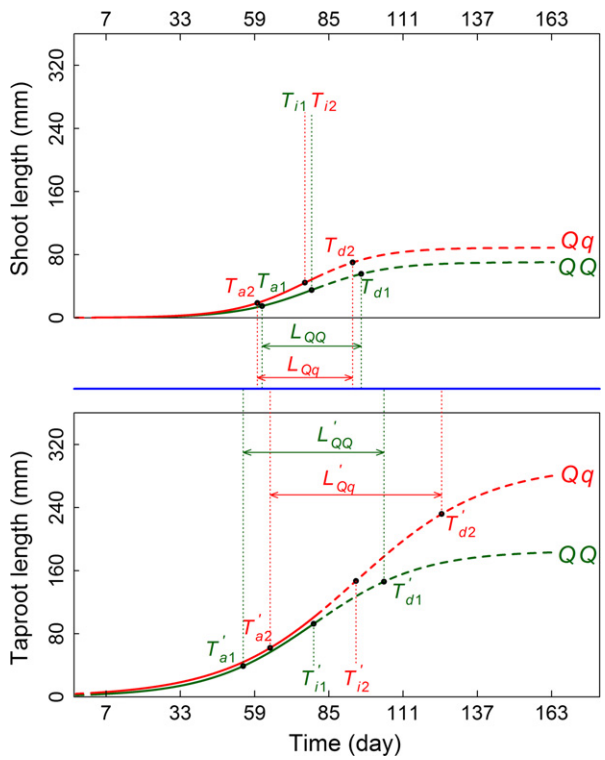

Figure 4. Growth curves of shoot and taproot lengths for two different genotypes at the quantitative trait loci (QTL) lm_ll_6547 on linkage group 5. The timing of inflection point and duration of linear growth are shown for each genotype. [Colour figure can be viewed at wileyonlinelibrary.com]

mapping context for identifying specific *h*QTLs that mediate growth allocation. From fundamental principles of biophysical and biochemical processes, logistic equations that capture different stages of organ development have been derived, which show robust biological relevance (West *et al.*, 2001). Sun *et al.* (2014) dissect logistic growth curves into several key landmarks of development using the concept of heterochrony, defined as the asymptotic growth, relative growth rate, the timing of inflection and the duration of linear growth. This concept has been successfully used to study the genetic architecture of leaf area and weight growth expressed in two contrasting environments in the common bean (Jiang *et al.*, 2015). From the analysis of phenotypic correlations, strong evidence has been observed for developmental modularity of the above- versus below-ground growth (El-Lithy *et al.*, 2010; Bai *et al.*, 2013). These heterochronic parameters were more tightly correlated within than between organs, but the interrelationships of these parameters are closer within the below- than above-ground parts, showing stronger modularity for the organ that plays a key role in resisting the adverse environment (El-Lithy *et al.*, 2010).

A further QTL analysis found that different sets of *h*QTLs were involved in the heterochronic variation of above- and below-ground growth, suggesting that these two modules had different genetic basis. It has been recognized that the distribution pattern of above- and below-ground biomass growth is under strong environmental impact in forest trees (Wullschleger *et al.*, 2005; Rae *et al.*, 2007; Novaes *et al.*, 2009). For example, the average above- to below-ground biomass ratio in an interspecific poplar pedigree was found to increase very rapidly with nitrogen availability (Novaes *et al.*, 2009). Thus, different genetic machineries of the two modules allow them to respond instantly when the environment changes. On the other hand, by a bivariate analysis, we also identified a couple of *h*QTLs that mediate pleiotropically the pattern of above- and below-ground growth. These pleiotropic *h*QTLs help Euphrates Poplars to maintain their functional equilibrium to better adapt to the arid environment of the dessert.

Through gene function annotation, 15 of the *h*QTLs mapped were detected to reside in the candidate genes. These genes code cation/H^+ antiporter (CHX24), protein phosphatase, nodulin family protein, mitochondrial RNA pseudouridine synthase (At3 g19440), polyadenylation and cleavage factor homolog 4-like (PCFS4), pentatricopeptide repeat-containing protein (LOI1, At4g14850), leucine-rich repeat receptor-like protein kinase PEPR1 (PEPR1) and F-box protein (At4g22030), which participate in cation transportation, protein phosphorylation, nodule formation, RNA synthase, mRNA maturation, isoprenoid biosynthesis, plant defense, hormone signal transduction and biological developmental processes (Tables 2 and 3). PCFS4 promotes flowering (Xing *et al.*, 2008) and mediates mRNA maturation (Zheng *et al.*, 2011). At4g22030 codes F-box protein, one of the three components of the SCF complex (Stone and Callis, 2007). As the mediator for ubiquitination protein degradation by the 26S proteasome (Vierstra, 2009), F-box protein is associated with cellular functions such as hormone signal transduction and regulation of the cell cycle (Craig and Tyers, 1999; Kepinski and Leyser, 2005). It also plays an important role in various biological processes, such as circadian clock regulation (Más *et al.*, 2003), self-incompatibility (Williams *et al.*, 2014), floral development (Levin and Meyerowitz, 1995), photomorphogenesis (Büche *et al.*, 2000; Imaizumi *et al.*, 2005) and plant stress response (Sijacic *et al.*, 2004; Bu *et al.*, 2013). PEPR1 located on linkage group 12 plays a key role in plant defense, as a receptor gene for PEP defense peptides (Yamaguchi *et al.*, 2006). LOI1 and At3 g19440 participate in the processes of isoprenoid biosynthesis (Kobayashi *et al.*, 2007) and RNA synthase of mitochondria, respectively. Both of them are detected to interact with multiple genes through protein–protein interactive network. These candidate genes are essential for cation transportation, protein phosphorylation, nodule formation, RNA synthase, mRNA maturation, isoprenoid biosynthesis, plant defense, hormone signal transduction and other biological

developmental processes during the period of seedlings growth and development.

Seedling performances at the germination stage are one of the most important aspects for plants to better grow and reproduce in their late stages, but our knowledge about the genetic basis of how shoot growth and root growth covary is limited. Our results highlight that the growth pattern of above- and below-group parts in Euphrates Poplars represent different developmental modules within which heterochronic parameters are correlated more strongly with each other but less strongly with those from a different module (Wagner *et al.*, 2007). Beyond this, our genetic mapping clearly demonstrates relatively different machineries between above- and below-ground growth modules, suggesting their different capacities to evolve. Further investigations are needed to confirm or modify our findings by QTL mapping in natural populations.

EXPERIMENTAL PROCEDURES

Mapping population

A full-sib F_1 population of 370 members was derived from a cross between two dioecious *P. euphratica* trees, which grow naturally in Korla, Xinjiang, China (85°14′10″−86°24′21″E, 41°10′48″−41°21′36″N). In spring 2014, male and female flowering branches, cut from these two selected trees, respectively, were cultivated in water for artificial hybridization. More than 4 months after pollination, the catkins entered gradually their ripening stage, at which the seeds were harvested and each cultivated in a glass tube (40 mm in diameter and 400 mm in length) under a sterile culture condition. The tube contains 350 ml 1/2 Murashige and Skoog medium (pH 6.0) laid out in a phytotron set at 14-h-day/10-h-night cycle, 28°C day and 22°C night with 800 μmol m^{-2} s^{-1} photosynthetically active radiation.

Phenotyping

Among all seeds reared in culture tubes, 35% have germinated and grown into seedlings, finally obtaining 370 normally growing progeny. The first observation time was individual-dependent, ranging from 6 to 23 days after being planted in glass tubes. Shoot length and taproot length were measured repeatedly for each progeny once every week until some fast-growing seedlings fill the tubes. In total, measurements were undertaken for about 3 months, totaling 12 or 16 times. The specific measurement time for each individual can be found in Figures S1 and S2. Because of differences in the emerging date of seedlings among progeny as well as the effort to reduce human measurement errors by limiting the number of measuring personnel, the schedules of measurement are slightly progeny-dependent. These uneven-spaced, progeny-dependent measurement schedules do not affect our subsequent estimates of curve parameters from a growth equation as the curve fitting was performed for individual progeny.

SNP genotyping

Leaf samples (3–5 g) of the two parents and 370 progeny were flash-frozen in liquid nitrogen and then stored at −80°C, respectively. All genomic DNA were extracted from leaves, using a DNA extraction kit (Tiangen, Beijing) following the manufacturer's protocol. DNA concentration and quality were determined by agarose gel electrophoresis and a Nanodrop 2000 spectrophotometer (Thermo Scientific, Wilmington, DE, USA). Restriction-site associated DNA (RAD) library construction, sample indexing and pooling were prepared following Baird *et al.* (2008). Based on a DNA digestion experiment by using various restriction enzymes, EcoRI was selected to cut the DNA. In total, 11 multiplexed sequencing libraries were constructed where each DNA sample was assigned a unique nucleotide multiplex identifier (MID) for barcoding. Single-end (101-bp) sequencing was performed using Illumina HiSeq2000 in a total throughput of four lanes. Raw sequence reads were trimmed to 85 nucleotides from the 3′ end to 5′ end through quality control, ensuring more than 90% of sequences reached Q30 (0.1% sequencing error) and more than 99% reached Q20 (1% sequencing error). Stacks (Catchen *et al.*, 2011) were used to produce unique candidate alleles for each RAD locus by clustering the trimmed reads into read tags (RAD-tags). Only one base-pair mismatch was allowed in this step. To avoid high linkage disequilibrium in the short RAD reads, only those with two haplotypes were retained. RAD-tags were then collapsed into clusters using Stacks under default parameters for SNP calling. RAD clusters with very high read depth (>500) were excluded from SNP calling. We called genotypes from the 370 F1 progeny by using a strict Bayesian method, and identified 5885 SNPs segregating in the mapping population. All the procedures followed the method used by Xu *et al.* (2014).

Statistical analysis

Linkage analysis. For a full-sib family derived from two heterozygous parents, there are two segregating types of markers: (1) testcross markers at which one parent is heterozygous while the other is homozygous; and (2) intercross markers at which both parents are heterozygous. Also, any marker pair of heterozygous parents has an unknown linkage phase, which affects linkage analysis from marker data of the full-sib family. Wu and his group have derived a statistical model that can simultaneously estimate the recombination fraction and the linkage phase of adjacent markers for any types of markers (testcross and intercross; Wu *et al.*, 2002; Lu *et al.*, 2004). This model has packed in OneMap software by Margarido *et al.* (2007), which was used to construct the genetic linkage map for our full-sib family. The Kosambi map function was used to convert the recombination fraction to map length. The total length of linkage map is 4574.89 cM, with the average map distance of 0.54 cM.

Curve fitting. This study will focus on shoot length and taproot length as indicators of above- and below-ground growth components, respectively. As a growth trait, shoot and root lengths can be fitted by a growth equation. We found that the time-serial observational data of these two traits can be fitted by a three-parameter growth equation, through a non-linear least-square approach, which is expressed as

$$g(t) = \frac{a}{1 + be^{-rt}} \quad (1)$$

where $g(t)$ is the trait value at time t, and three parameters a, b and r have different biological meanings: a is the limit value of g when $t \to \infty$, r is the relative growth rate, and $a/(1 + b)$ denotes the initial value of g when $t = 0$. After the three growth parameters were estimated for each progeny, we further determined heterochronic parameters, i.e. the timing of inflection point (t_i), the timing of maximum acceleration (t_a), the timing of maximum deceleration (t_d) and the duration of linear growth (L) (Sun *et al.*, 2014).

QTL mapping

For each progeny, we estimated a series of heterochronic parameters using equation (1), and then treated these estimates as phenotypic values to perform QTL mapping. There are two statistical approaches for QTL mapping, mixture model for sparse molecular markers and multiplicative model for dense markers. Because the linkage map constructed is quite dense, we employed the multiplicative model that assumes QTLs are located at the positions of markers. For the same heterochronic parameter expressed in shoot length and taproot length, the multiplicative likelihood model is expressed as

$$L(\phi|\mathbf{y}) = \prod_{i=1}^{n_1} f_1(\mathbf{y}_i)\ldots\prod_{i=1}^{n_J} f_J(\mathbf{y}_i) \quad (2)$$

where Φ is the unknown parameters; $\mathbf{y}_i = (y_{1i}, y_{2i})$ is the growth parameter vector of progeny i for shoot length (coded by 1) and taproot length (coded by 2); n_j is the number of progeny with SNP genotype j; and $f_j(\mathbf{y}_i)$ is a bivariate normal distribution for progeny i with the expected mean vector for genotype j (μ_{1j}, μ_{2j}) and the variance-covariance matrix Σ containing the variances (σ_1^2, σ_2^2) and correlation between the two traits (ρ). Statistical methods based on the likelihood (2) have been established to estimate the model parameters $\Phi = (\mu_{1j}, \mu_{2j}, \sigma_1^2, \sigma_2^2, \rho)$.

Hypothesis tests

It is important to test whether and how a QTL affects the heterochronic variation of shoot length and taproot length, and their covariation through developmental mechanisms. The first hypothesis is about the existence of so-called *h*QTLs, which can be tested by the null hypothesis H_0: (μ_{1j}, μ_{2j}) ((μ_1, μ_2). By comparing its likelihood with that of the alternative hypothesis, we calculated the log-likelihood ratio, from which to calculate the *P*-value for each marker. We used Bonferroni correction to adjust for multiple comparisons given the number of markers analyzed.

The second hypothesis is about the common genetic basis of above- and below-ground traits. The same *h*QTL may pleiotropically affect different traits. This can be tested by building the null hypotheses, H_0: μ_{1j} (μ_1 and H_0: $\mu_{2j} \equiv \mu_2$. If both are rejected, then this means that the *h*QTL triggers a pleiotropic effect on both traits (Jiang and Zeng, 1995; Neto *et al.*, 2008). Otherwise, the *h*QTL is trait-specific; i.e. its expression depends on the trait.

All the data analyses including curve fitting, QTL mapping and correlations analysis were performed in R version 3.3.1 (R Core Team, 2015). Possible functions for all *h*QTLs determined were annotated and predicted via BLAST in the 'nr' database on National Center of Biotechnology Information website (NCBI; http://blast.ncbi.nlm.nih.gov/), identified on Uniprot (http://www.uniprot.org/), and analyzed for protein–protein interaction network using online protein interactions analysis software STRING (http://string-db.org/).

ACKNOWLEDGEMENTS

This work is supported by the grant 201404102 from the State Administration of Forestry of China, the Changjiang Scholars Award and 'One-thousand Person Plan' Award.

CONFLICTS OF INTEREST

The authors declare no conflicts of interest.

SUPPORTING INFORMATION

Additional Supporting Information may be found in the online version of this article.

Figure S1. The fitness of growth equation to observational data of shoot length for individual seedlings.

Figure S2. The fitness of growth equation to observational data of taproot length for individual seedlings.

Figure S3. The residuals of fitted growth equation for shoot length and taproot length over time.

Figure S4. Significance tests of SNPs for different heterochronic parameters by univariate and bivariate models.

Table S1 The parameters for 370 seedlings in F_1 population of *P. euphratica* for shoot length and taproot root length

Table S2 Annotation of genes that interact with At3 g19440 and LOI1 in *A. thaliana*

Table S3 Functional enrichments of At3 g19440 and LOI1 in *A. thaliana*

REFERENCES

Anithakumari, A., Dolstra, O., Vosman, B., Visser, R.G. and van der Linden, C.G. (2011) In vitro screening and QTL analysis for drought tolerance in diploid potato. *Euphytica*, **181**, 357–369.

Bai, C., Liang, Y. and Hawkesford, M.J. (2013) Identification of QTLs associated with seedling root traits and their correlation with plant height in wheat. *J. Exp. Bot.* **64**, 1745–1753.

Baird, N.A., Etter, P.D., Atwood, T.S., Currey, M.C., Shiver, A.L., Lewis, Z.A., Selker, E.U., Cresko, W.A. and Johnson, E.A. (2008) Rapid SNP discovery and genetic mapping using sequenced RAD markers. *PLoS ONE*, **3**, e3376.

Baker, R.L., Leong, W.F., Brock, M.T., Markelz, R.J., Covington, M.F., Devisetty, U.K., Edwards, C.E., Maloof, J., Welch, S. and Weinig, C. (2015) Modeling development and quantitative trait mapping reveal independent genetic modules for leaf size and shape. *New Phytol.* **208**, 257–268.

Bouteille, M., Rolland, G., Balsera, C., Loudet, O. and Muller, B. (2012) Disentangling the intertwined genetic bases of root and shoot growth in Arabidopsis. *PLoS ONE*, **7**, e32319.

Brouwer, R. (1963) Some aspects of the equilibrium between overground and underground plant parts. *Jaarboek van het Instituut Voor Biologisch en Scheikundig Onderzoek aan Landbouwgewassen*, **1963**, 31–39.

Bu, Q., Lv, T., Shen, H. *et al.* (2013) Regulation of drought tolerance by the F-Box protein MAX2 in Arabidopsis. *Plant Physiol.* **164**, 424–439.

Büche, C., Poppe, C., Schäfer, E. and Kretsch, T. (2000) eid1: a new Arabidopsis mutant hypersensitive in phytochrome A-dependent high-irradiance responses. *Plant Cell*, **12**, 547–558.

Catchen, J.M., Amores, A., Hohenlohe, P., Cresko, W. and Postlethwait, J.H. (2011) Stacks: building and genotyping Loci de novo from short-read sequences. *G3: Genes - Genomes - Genetics*, **1**, 171–182.

Chen, X., Yao, Q., Gao, X., Jiang, C., Harberd, N.P. and Fu, X. (2016) Shoot-to-root mobile transcription factor HY5 coordinates plant carbon and nitrogen acquisition. *Curr. Biol.* **26**, 640–646.

Craig, K.L. and Tyers, M. (1999) The F-box: a new motif for ubiquitin dependent proteolysis in cell cycle regulation and signal transduction. *Prog. Biophys. Mol. Bio.* **72**, 299–328.

El-Lithy, M.E., Reymond, M., Stich, B., Koornneef, M. and Vreugdenhil, D. (2010) Relation among plant growth, carbohydrates and flowering time in the Arabidopsis Landsberg erecta x Kondara recombinant inbred line population. *Plant, Cell Environ.* **33**, 1369–1382.

Ferreira, S., Batista, D., Serrazina, S. and Pais, M.S. (2008) Morphogenesis induction and organogenic nodule differentiation in *Populus euphratica* Oliv. leaf explants. *Plant Cell Tiss. Org.* **96**, 35–43.

Gartner, B.L. (1995) *Plant Stems: Physiology and Functional Morphology*. San Diego: Academic Press.

He, Q., Berg, A., Li, Y., Vallejos, C.E. and Wu, R. (2010) Mapping genes for plant structure, development and evolution: functional mapping meets ontology. *Trends Genet.* **26**, 39–46.

Hernandez, K.M. (2015) Understanding the genetic architecture of complex traits using the function-valued approach. *New Phytol.* **208**, 1–3.

Hou, W., Garvan, C.W., Zhao, W., Behnke, M., Eyler, F.D. and Wu, R. (2005) A general model for detecting genetic determinants underlying longitudinal traits with unequally spaced measurements and nonstationary covariance structure. *Biostatistics*, **6**, 420–433.

Hou, W., Garvan, C.W., Littell, R.C., Behnke, M., Eyler, F.D. and Wu, R. (2006) A framework to monitor environment-induced major genes for developmental trajectories: implication for a prenatal cocaine exposure study. *Stat. Med.* **25**, 4020–4035.

Imaizumi, T., Schultz, T.F., Harmon, F.G., Ho, L.A. and Kay, S.A. (2005) FKF1 F-box protein mediates cyclic degradation of a repressor of *CONSTANS* in *Arabidopsis*. *Science*, **309**, 293–297.

Jiang, C. and Zeng, Z.B. (1995) Multiple trait analysis of genetic mapping for quantitative trait loci. *Genetics*, **140**, 1111–1127.

Jiang, L., Clavijo, J.A., Sun, L., Zhu, X., Bhakta, M.S., Gezan, S.A., Carvalho, M., Vallejos, C.E. and Wu, R. (2015) Plastic expression of heterochrony quantitative trait loci (hQTLs) for leaf growth in the common bean (*Phaseolus vulgaris*). *New Phytol.* **207**, 872–882.

Kepinski, S. and Leyser, O. (2005) The Arabidopsis F-box protein TIR1 is an auxin receptor. *Nature*, **435**, 446–451.

Khan, M.A., Saravia, D., Munive, S., Lozano, F., Farfan, E., Eyzaguirre, R. and Bonierbale, M. (2015) Multiple QTLs linked to agro-morphological and physiological traits related to drought tolerance in potato. *Plant Mol. Biol. Report*, **33**, 1286–1298.

Kobayashi, K., Suzuki, M., Tang, J. *et al.* (2007) Lovastatin insensitive 1, a Novel pentatricopeptide repeat protein, is a potential regulatory factor of isoprenoid biosynthesis in *Arabidopsis*. *Plant Cell Physiol.* **48**, 322–331.

Lander, E.S. and Botstein, D. (1989) Mapping mendelian factors underlying quantitative traits using RFLP linkage maps. *Genetics*, **121**, 185–199.

Levin, J.Z. and Meyerowitz, E.M. (1995) UFO: an Arabidopsis gene involved in both floral meristem and floral organ development. *Plant Cell*, **7**, 529–548.

Li, Z. and Sillanpaa, M.J. (2015) Dynamic quantitative trait locus analysis of plant phenomic data. *Trends Plant Sci.* **20**, 822–833.

Li, Y. and Wu, R. (2010) Functional mapping of growth and development. *Biol. Rev.* **85**, 207–216.

Liu, Y., Li, X., Chen, G., Li, M., Liu, M. and Liu, D. (2015) Epidermal micromorphology and mesophyll structure of *Populus euphratica* heteromorphic leaves at different development stages. *PLoS ONE*, **10**, e0137701.

Lu, Q., Cui, Y. and Wu, R. (2004) A multilocus likelihood approach to joint modeling of linkage, parental diplotype and gene order in a full-sib family. *BMC Genet.* **5**, 20.

Ma, C.-X., Casella, G. and Wu, R. (2002) Functional mapping of quantitative trait loci underlying the character process: a theoretical framework. *Genetics*, **161**, 1751–1762.

Margarido, G.R., Souza, A.P. and Garcia, A.A. (2007) OneMap: software for genetic mapping in outcrossing species. *Hereditas*, **144**, 78–79.

Más, P., Kim, W.-Y., Somers, D.E. and Kay, S.A. (2003) Targeted degradation of TOC1 by ZTL modulates circadian function in *Arabidopsis thaliana*. *Nature*, **426**, 567–570.

Miles, C. and Wayne, M. (2008) Quantitative trait locus (QTL) analysis. *Nature Educat.* **1**, 208.

Muraya, M.M., Chu, J., Zhao, Y., Junker, A., Klukas, C., Reif, J.C. and Altmann, T. (2017) Genetic variation of growth dynamics in maize (*Zea mays* L.) revealed through automated non-invasive phenotyping. *Plant J.* **89**, 366–380.

Naz, A.A., Arifuzzaman, M., Muzammil, S., Pillen, K. and Leon, J. (2014) Wild barley introgression lines revealed novel QTL alleles for root and related shoot traits in the cultivated barley (*Hordeum vulgare* L.). *BMC Genet.* **15**, 107.

Neto, E.C., Ferrara, C.T., Attie, A.D. and Yandell, B.S. (2008) Inferring causal phenotype networks from segregating populations. *Genetics*, **179**, 1089–1100.

Novaes, E., Osorio, L., Drost, D.R. *et al.* (2009) Quantitative genetic analysis of biomass and wood chemistry of Populus under different nitrogen levels. *New Phytol.* **182**, 878–890.

Paul, M.J. and Foyer, C.H. (2001) Sink regulation of photosynthesis. *J. Exp. Bot.* **52**, 1383–1400.

Poorter, H., Niklas, K.J., Reich, P.B., Oleksyn, J., Poot, P. and Mommer, L. (2012) Biomass allocation to leaves, stems and roots: meta-analyses of interspecific variation and environmental control. *New Phytol.* **193**, 30–50.

R Core Team (2015) *R: A Language and Environment for Statistical Computing*. R Vienna, Austria: Foundation for Statistical Computing, URL https://www.R-project.org/.

Rae, A.M., Tricker, P.J., Bunn, S.M. and Taylor, G. (2007) Adaptation of tree growth to elevated CO2: quantitative trait loci for biomass in Populus. *New Phytol.* **175**, 59–69.

Reich, P.B. (2002) Root-shoot relations: optimality in acclimation and adaptation or the "emperor's new clothes". In *Plant roots: the hidden half*, 3rd edn (Waisel, Y., Eshel, A., Beeckman, T. and Kafkafi, U., eds). New York: Marcel Dekker, Inc., pp. 205–220.

Ruta, N., Stamp, P., Liedgens, M., Fracheboud, Y. and Hund, A. (2010) Collocations of QTLs for seedling traits and yield components of tropical maize under water stress conditions. *Crop Sci.* **50**, 1385–1392.

Shipley, B. and Meziane, D. (2002) The balanced-growth hypothesis and the allometry of leaf and root biomass allocation. *Funct. Ecol.* **16**, 326–331.

Si, J., Zhou, T., Bo, W., Xu, F. and Wu, R. (2014) Genome-wide analysis of salt-responsive and novel microRNAs in *Populus euphratica* by deep sequencing. *BMC Genet.* **15**(Suppl 1), S6.

Sijacic, P., Wang, X., Skirpan, A.L., Wang, Y., Dowd, P.E., McCubbin, A.G., Huang, S. and Kao, T.-H. (2004) Identification of the pollen determinant of S-RNase-mediated self-incompatibility. *Nature*, **429**, 302–305.

Stone, S.L. and Callis, J. (2007) Ubiquitin ligases mediate growth and development by promoting protein death. *Curr. Opin. Plant Biol.* **10**, 624–632.

Sun, L. and Wu, R. (2015) Mapping complex traits as a dynamic system. *Phys. Life Rev.* **13**, 155–185.

Sun, L., Ye, M., Hao, H., Wang, N., Wang, Y., Cheng, T., Zhang, Q. and Wu, R. (2014) A model framework for identifying genes that guide the evolution of heterochrony. *Mol. Biol. Evol.* **31**, 2238–2247.

Verma, G., Mishra, S., Sangwan, N. and Sharma, S. (2015) Reactive oxygen species mediate axis-cotyledon signaling to induce reserve mobilization during germination and seedling establishment in Vigna radiata. *J. Plant Physiol.* **184**, 79–88.

Vierstra, R.D. (2009) The ubiquitin–26S proteasome system at the nexus of plant biology. *Nature Rev. Mol. Cell Biol.* **10**, 385–397.

Wagner, G.P., Pavlicev, M. and Cheverud, J.M. (2007) The road to modularity. *Nat. Rev. Genet.* **8**, 921–931.

Wang, L., Zhao, C., Li, J., Liu, Z. and Wang, J. (2015) Root plasticity of *Populus euphratica* seedlings in response to different water table depths and contrasting sediment types. *PLoS ONE*, **10**, e0118691.

West, G.B., Brown, J.H. and Enquist, B.J. (2001) A general model for ontogenetic growth. *Nature*, **413**, 628–631.

Williams, J.S., Der, J.P. and Kao, T.-H. (2014) Transcriptome analysis reveals the same 17 S-locus F-box genes in two haplotypes of the self-incompatibility locus of *Petunia inflata*. *Plant Cell*, **26**, 2873–2888.

Wu, R.L. and Lin, M. (2006) Opinion – functional mapping – how to map and study the genetic architecture of dynamic complex traits. *Nature Rev. Genet.* **7**, 229–237.

Wu, R., Ma, C.-X., Painter, I. and Zeng, Z.-B. (2002) Simultaneous maximum likelihood estimation of linkage and linkage phases in outcrossing species. *Theor. Popul. Biol.* **61**, 349–363.

Wu, R., Ma, C. and Casella, G. (2007) *Statistical Genetics of Quantitative Traits: Linkage, Maps and QTL*. New York: Springer-Verlag.

Wullschleger, S.D., Yin, T.M., DiFazio, S.P., Tschaplinski, T.J., Gunter, L.E., Davis, M.F. and Tuskan, G.A. (2005) Phenotypic variation in growth and biomass distribution for two advanced-generation pedigrees of hybrid poplar. *Can. J. Forest Res.* **35**, 1779–1789.

Xing, D., Zhao, H., Xu, R. and Li, Q.Q. (2008) Arabidopsis PCFS4, a homologue of yeast polyadenylation factor Pcf11p, regulates *FCA* alternative processing and promotes flowering time. *Plant J.* **54**, 899–910.

Xu, P., Xu, S., Wu, X., Tao, Y., Wang, B., Wang, S., Qin, D., Lu, Z. and Li, G. (2014) Population genomic analyses from low-coverage RAD-Seq data: a case study on the non-model cucurbit bottle gourd. *Plant J.* **77**, 430–442.

Yamaguchi, Y., Pearce, G. and Ryan, C.A. (2006) The cell surface leucine-rich repeat receptor for AtPep1, an endogenous peptide elicitor in *Arabidopsis*, is functional in transgenic tobacco cells. *Proc. Natl Acad. Sci. USA*, **103**, 10104–10109.

Zheng, J., Xing, D., Wu, X., Shen, Y., Kroll, D.M., Ji, G. and Li, Q.Q. (2011) Ratio-based analysis of differential mRNA processing and expression of a polyadenylation factor mutant *pcfs4* using arabidopsis tiling microarray. *PLoS ONE*, **6**, e14719.